Untangling TMS-EEG responses caused by TMS *versus* sensory input using optimized sham control and GABAergic challenge

Pedro C. Gordon[1,2], Yu Fei Song[1,2], D. Blair Jovellar[1,2], Maryam Rostami[3] , Paolo Belardinelli[1,2,4] and Ulf Ziemann[1,2]

[1]*Department of Neurology & Stroke, University of Tübingen, Tübingen, Germany*
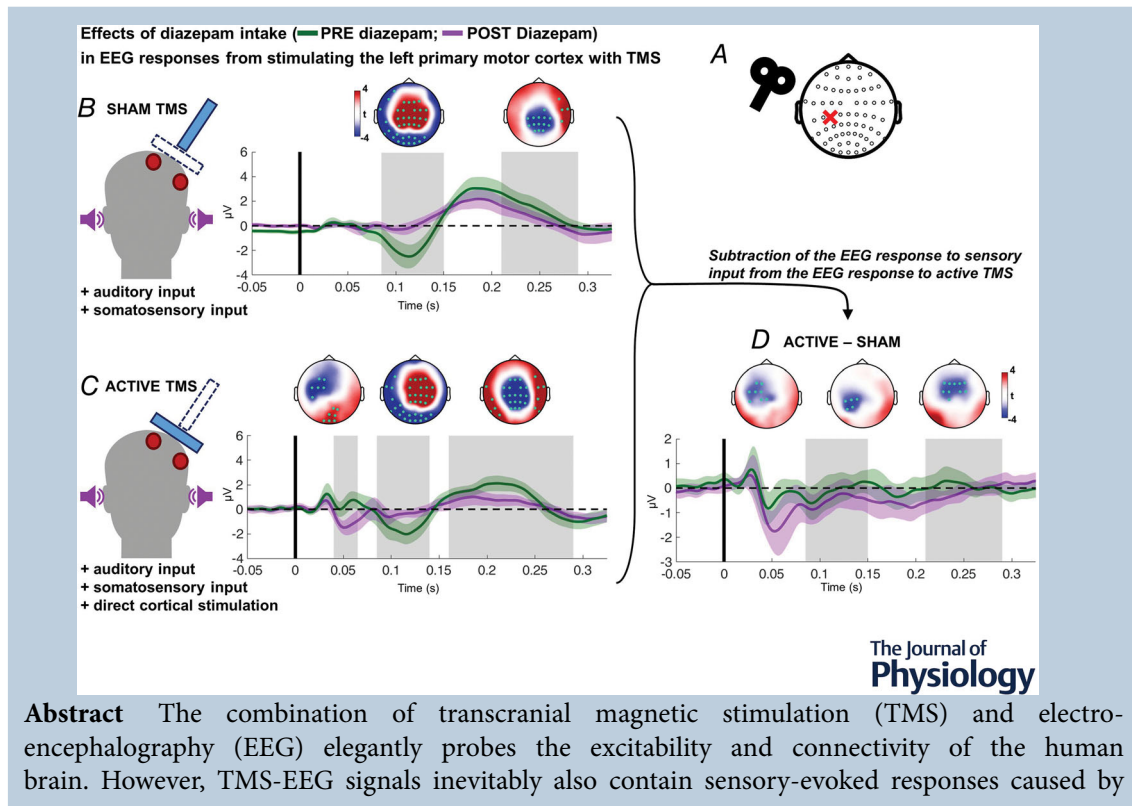[2]*Hertie Institute for Clinical Brain Research, University of Tübingen, Tübingen, Germany*
[3]*Faculty of Electrical and Computer Engineering, University of Tehran, Tehran, Iran*
[4]*CIMeC, Center for Mind/Brain Sciences, University of Trento, Trento, Italy*

Handling Editors: Richard Carson & Charlotte Stagg

The peer review history is available in the Supporting information section of this article (https://doi.org/10.1113/JP283986#support-information-section).

Effects of diazepam intake (— PRE diazepam; — POST Diazepam) in EEG responses from stimulating the left primary motor cortex with TMS

B SHAM TMS
+ auditory input
+ somatosensory input

A

C ACTIVE TMS
+ auditory input
+ somatosensory input
+ direct cortical stimulation

Subtraction of the EEG response to sensory input from the EEG response to active TMS

D ACTIVE – SHAM

Abstract The combination of transcranial magnetic stimulation (TMS) and electro-encephalography (EEG) elegantly probes the excitability and connectivity of the human brain. However, TMS-EEG signals inevitably also contain sensory-evoked responses caused by

Pedro C. Gordon Medical degree at the University of Sao Paulo, Brazil, 2009. Psychiatry specialty at the faculty of medicine of the University of Sao Paulo, Brazil, 2012. Master of science degree at the faculty of medicine of the University of Sao Paulo, Brazil, 2014. Doctor of science degree at the faculty of medicine of the University of Sao Paulo, Brazil, 2018. Postdoctoral researcher at the department of neurology of the University of Tübingen, Germany, since 2018.

TMS-associated auditory and somatosensory inputs, constituting a substantial confounding factor. Here we applied our recently established optimized SHAM protocol (Gordon et al., Neuroimage 2021:118708) to disentangle TMS-EEG responses caused by TMS *vs.* sensory input. One unresolved question is whether these responses superimpose without relevant interaction, a requirement for their disaggregation by the optimized SHAM approach. We applied in 20 healthy subjects a pharmacological intervention using a single oral dose of 20 mg of diazepam, a positive modulator of GABAA receptors. Diazepam decreased the amplitudes of the P60 and P150 components specifically in the ACTIVE TMS and/or the ACTIVE TMS minus SHAM conditions but not in the SHAM condition, pointing to a response caused by TMS. In contrast, diazepam suppressed the amplitude of the N100 component indiscriminately in the ACTIVE TMS and SHAM conditions but not in the ACTIVE TMS minus SHAM condition, pointing to a response caused by sensory input. Moreover, diazepam suppressed the beta-band response observed in the motor cortex specifically after ACTIVE TMS and ACTIVE TMS minus SHAM. These findings demonstrate a lack of interaction of TMS-EEG responses caused by TMS *vs.* sensory input and validate optimized SHAM-controlled TMS-EEG as an appropriate approach to untangle these TMS-EEG responses. This knowledge will enable the proficient use of TMS-EEG to probe the physiology of the human cortex.

Corresponding author Ulf Ziemann: Department of Neurology & Stroke, Hoppe-Seyler-Straße 3, 72076 Tübingen, Germany.   Email: ulf.ziemann@uni-tuebingen.de

Abstract figure legend *A*, representation of the transcranial magnetic stimulation (TMS) target on the scalp (marked as red 'x') indicating the left primary motor cortex (around the location of the C3 electrode). *B*, representation of the SHAM TMS condition, which involved the delivery of auditory (masking nose and sham coil) and somatosensory stimuli (scalp electrical stimulation) of equivalent intensity compared with the ACTIVE TMS. To the right, topographical plots display the results from the statistical comparison between responses post- *vs.* pre-diazepam intake, using cluster-based dependent sample *t* tests (electrodes that comprised the significant clusters in cyan). Below, time-course plot of the EEG responses to the stimuli before (green) and after (purple) the intake of diazepam. Plotted signal corresponds to the average across all significant electrodes, displayed in the topographical plots above. Shaded grey areas indicate the time windows of significant difference between the EEG responses. *C*, representation of the ACTIVE TMS condition, which, in addition to auditory (masking noise and real coil) and somatosensory stimuli (scalp electrical stimulation and real coil), involved the direct activation of the underlying cortex. Time-course plot of EEG responses and topographical plots as in *B*. *D*, by subtracting the individual EEG responses to sensory stimuli (SHAM) from the response to TMS (ACTIVE) we obtain the EEG response attributed solely to the direct cortical activation by TMS. Time-course plot of EEG responses and topographical plots as in *B*.

Key points

- Optimized SHAM disentangles TMS-EEG responses caused by TMS *vs.* sensory input.
- Diazepam differentially modulates TMS-EEG responses caused by TMS *vs.* sensory input.
- Diazepam modulation of P60 and P150 indicate TMS-EEG responses caused by TMS.
- Diazepam modulation of N100 indicate a TMS-EEG response caused by sensory input.

Introduction

The combined use of transcranial magnetic stimulation (TMS) and electroencephalography (EEG) has gained significant attraction as a tool for understanding human neurophysiology (Chung et al., 2015; Tremblay et al., 2019). The technique involves non-invasive brain stimulation with TMS and simultaneous recording of cortical responses using scalp EEG, and provides information on neuronal excitability and connectivity of the stimulated region (Ilmoniemi & Kicic, 2010). TMS-EEG can potentially probe any region on the convexity of the cerebral cortex, obtaining EEG response signatures as markers of cortical responsivity (TMS-evoked potentials, TEPs). The TEP components are commonly referred to as typical positive (P) or negative (N) deflections following the TMS pulse in milliseconds (e.g. P30, N45, P60, N100 and P180 when probing the motor cortex) (Komssi et al., 2004; Lioumis et al., 2009).

Experiments combining TMS-EEG and neuropharmacology have helped to understand the neurophysiological mechanisms involved in TEPs (Darmani & Ziemann, 2019; Ziemann et al., 2015). By measuring TEPs prior to and following the intake of a central nervous system-active drug with a known specific mode of action, it is possible to infer that this mode of action contributes to the TEP components if they are significantly modified by the drug. Positive allosteric modulators of the GABAA receptors (GABAARs), i.e. benzodiazepines and zolpidem, increased the amplitude of the N45 and decreased the N100, whereas the GABABR agonist baclofen increased the N100 amplitude (Premoli et al., 2014). These findings imply that GABAAergic mechanisms contribute to the N45, while the N100 represents a more complex interaction of GABAAergic and GABABergic systems (Premoli et al., 2014). Similar to the positive allosteric modulators of the GABAAR, the antiglutamatergic *N*-methyl-ᴅ-aspartate receptor antagonist dextromethorphan increased the N45 amplitude, reinforcing the notion that TMS-EEG responses reflect the state of an excitation/inhibition balance under the control of glutamatergic/GABAergic dynamics (Belardinelli et al., 2021). These and similar other pharmaco-TMS-EEG studies have been important in establishing a neurophysiological basis for further TMS-EEG findings, including its use in the search for potential biomarkers for neuropsychiatric disorders. For instance, TMS-EEG revealed an abnormally low N100 amplitude in patients with attention deficit hyperactivity disorder (ADHD) and schizophrenia, which is in line with models of impaired cortical inhibition secondary to GABAergic dysregulation in these disorders (Bruckmann et al., 2012; Noda et al., 2018).

However, it is known that TMS inevitably generates considerable multisensory input leading to evoked EEG responses (peripherally evoked potentials – PEPs), which overlap with the EEG response from direct cortical activation by TMS, a caveat that has already been identified in early TMS-EEG studies (Nikouline et al., 1999; Paus et al., 2001). This multisensory input includes a high-pitched 'click' sound generated during coil discharge, and somatosensory stimulation of the scalp near the targeted area (Ilmoniemi & Kicic, 2010). This raises the question as to what extent TMS-EEG reflects responses to direct cortical activation by TMS or to the TMS-associated multisensory inputs. If the latter were true, then changes in TMS-EEG responses caused by a neuromodulatory intervention, as well as TMS-EEG response abnormalities in neuropsychiatric disorders, may reflect changes in PEPs rather than TEPs. This would significantly undermine the potential of TMS-EEG to investigate focal brain responsivity.

Here we aimed to test to what extent changes in TMS-EEG responses caused by a single oral dose of a positive allosteric modulator of the GABAAR (diazepam) can be attributed to the modulation of TEPs or PEPs. This investigation is enabled by a newly developed optimized SHAM protocol in TMS-EEG measures, which allows the extraction of TMS-EEG responses that are cleaned from PEPs (Gordon et al., 2021). The rationale of the optimized SHAM was to apply auditory masking, identical auditory input as in ACTIVE TMS, and high-intensity electrical stimulation (ES) of the scalp to saturate somatosensory-evoked potentials. Auditory masking and ES were also applied in ACTIVE TMS. We proposed that ACTIVE TMS minus SHAM responses would reflect true TEPs, under the assumption that TEPs and PEPs are largely independent, i.e. do not non-linearly interact with each other (Gordon et al., 2021). This assumption has been made stronger by the observation that TEPs are not modulated by changing levels of sensory input (Gordon et al., 2023). Therefore, it is possible to identify the modulatory effect of a given intervention over TEPs from the effects over PEPs by isolating these components before and after the intervention. We then tested the existence of modulatory effects of diazepam specifically on components of the ACTIVE TMS minus SHAM response and, at the same time, modulatory effects indiscriminately on other components of ACTIVE TMS and SHAM responses. If true, this would provide evidence of the different effects of neuromodulatory interventions (here a positive allosteric modulator at GABAARs) on EEG responses to sensory inputs and TMS cortical activation, as well as the possibility of disaggregating these responses by the optimized SHAM approach.

Methods

Subjects and design

The study included right-handed healthy volunteers (confirmed by the Edinburgh Handedness Inventory (Oldfield, 1971)) aged between 18 and 50 years for a two-session experiment. Exclusion criteria were: a history or presence of psychiatric or neurological diseases, intake of medication acting on the central nervous system, a history or presence of alcohol or illicit drug abuse, current pregnancy or breastfeeding, and resting motor threshold (RMT) >60% of the maximum stimulator output. This RMT limit was set because higher intensities would involve higher sensory input and potentially compromise the optimized sham procedure (Gordon et al., 2021). Ultimately, no subject was excluded due to this criterion.

A total of 23 subjects were initially included in the study. However, two subjects did not attend the second session and one subject presented a low-quality EEG signal due to excessive movement, preventing further analysis. Therefore, the final analysis included 20 subjects (14 female), with a mean age of 25.5 years (SD ± 4.7). The

study was approved by the ethics committee of the medical faculty of the University of Tübingen (456/2019BO2), conformed to the *Declaration of Helsinki*, and all subjects provided written informed consent prior to enrolment.

The study involved two experimental sessions separated by at least 1 week. Each experimental session involved a pre-intervention measurement with resting-state EEG and single-pulse TMS-EEG, followed by the pharmacological intervention, and then a post-intervention TMS-EEG measurement, identical to the pre-intervention measurement.

Intervention

The pharmacological intervention consisted of the intake of the positive allosteric modulator of the GABAAR diazepam (20 mg diazepam-ratiopharm). We included a control intervention with placebo (P-Tabletten Lichtenstein) in order to clarify that results are specifically due to pharmacological effects, although several studies have consistently confirmed that placebo intake does not result in any significant change in TMS-EEG responses (Belardinelli et al., 2021; Darmani et al., 2019; Premoli et al., 2014; Premoli, Biondi et al., 2017). All subjects received both diazepam and placebo interventions, each assigned to one of the two separate experimental sessions. The order in which the interventions were applied was pseudo-randomized and balanced across subjects. Both experimenters and subjects were blinded to the intervention, as diazepam and placebo tablets were highly similar in appearance and their package labels were covered and replaced by a code that mapped each session to an allocation table, which remained concealed until the end of the study. Drug intake occurred immediately after the pre-intervention measurements. A 60 min waiting time was then inserted prior to the post-intervention measurements in order to allow the plasma peak of diazepam to be reached (Shader et al., 1984).

Experimental set-up

Prior to the TMS-EEG sessions, subjects underwent magnetic resonance imaging (MRI) using a 3T Siemens PRISMA scanner to obtain T1-weighted anatomical images. MRI was used for proper positioning of the TMS coil with respect to the individual's brain anatomy, using a neuronavigation system (Localite GmbH, Sankt Augustin, Germany), and also for the EEG forward model and source reconstruction, explained below.

The experiment was conducted in a quiet room with subjects sitting comfortably on a reclined chair and instructed to keep their eyes open during the measurements. Scalp EEG was recorded from a TMS-compatible 64-channel Ag/AgCl sintered ring electrode cap (EasyCap GmbH, Germany) using a TMS-compatible EEG system and amplifiers (Bittium NeurOne, Finland). Electrode FCz was used as reference. Additionally, surface EMG was recorded through bipolar EMG adhesive hydrogel electrodes (Kendall, Covidien) from the abductor pollicis brevis (APB) and first dorsal interosseus (FDI) muscles of the right hand in a bipolar belly-tendon montage. EEG and EMG data were sampled at 5 kHz, and a 0.16–1.25 kHz bandpass filter was applied. EMG was used to determine RMT with standard methods (Groppa et al., 2012), using neuronavigation to guide the coil's position. The cortical target over the hand area of the left primary motor cortex (M1) that consistently elicited the largest motor-evoked potentials (MEPs) was defined as the hot spot. TMS was delivered using a figure-of-eight coil (external diameter of each wing, 90 mm) connected to a Magstim 200^2 magnetic stimulator (Magstim Company Ltd., UK) with a monophasic current waveform. The induced electrical field in the cortex was directed from lateral-posterior to medial-anterior. Two identical stimulators and coils were used in this experiment, one for the ACTIVE TMS condition and the other for the SHAM TMS condition (Fig. 1*A*). ES of the scalp, as part of the optimized SHAM procedure, was delivered by a Digitimer DS7A electric stimulator (Digitimer Ltd. UK) (Fig. 1*B*) (Gordon et al., 2021).

Resting-state EEG and TMS-EEG

Each pre- and post-intervention measurement included an eyes-open resting-state EEG and a single-pulse TMS-EEG. Resting-state EEG was recorded for 5 min. Subjects were comfortably seated, and instructed to fixate on a black cross 1 m in front of them.

The single-pulse TMS-EEG measurements consisted of 320 TMS pulses, 160 ACTIVE TMS and 160 SHAM TMS, randomly intermixed and applied with an intertrial interval of 3 s (± 1 s jitter). Throughout the TMS-EEG measurements, masking noise was delivered through earbuds, set to an intensity high enough to conceal the TMS click noise, or to reach the subject's discomfort threshold. The masking noise was designed to have the same spectral distribution as the coil click sound (Massimini et al., 2005).

The ACTIVE TMS coil was placed tangentially to the scalp and targeted the motor hot spot (Fig. 1*A*). The intensity used for ACTIVE TMS was 90% of RMT. This subthreshold intensity was chosen to avoid somatosensory input via re-afferent feedback from MEP-related muscle twitches (Fecchio et al., 2017; Petrichella et al., 2017), while being sufficient to elicit TEPs (Fecchio et al., 2017; Komssi & Kahkonen, 2006). EMG was recorded during the TMS-EEG measurements to ensure that no MEPs occurred. SHAM TMS involved the application of a click

sound jointly with scalp ES (Fig. 1*A*). This click sound was delivered by the SHAM coil placed atop the ACTIVE TMS coil but angled perpendicular to the scalp, in order to keep the induced electrical field away from the cortex, while still generating the characteristic click sound (Fig. 1*A*). The intensity of SHAM TMS was set to match the auditory sound pressure level of ACTIVE TMS at the ear canals (Gordon et al., 2021).

The optimized SHAM procedure involved ES of the scalp delivered by two pairs of 1 cm diameter electrodes placed between the EEG electrodes: two electrodes of the same polarity at the positions corresponding to FFT9h and AFF5h, according to the International 10−20 system for EEG, and two electrodes of opposite polarity at CPP3h and TPP7h (Fig. 1*B*). Electrode polarity was switched after each pulse to avoid charge accumulation. This array of stimulation electrodes was designed to match the perception of somatosensory input of the TMS pulses, which involves a rather wide area of sensation over the scalp (Conde et al., 2019) and cranial muscle twitches around the target. Importantly, ES was applied in both the ACTIVE TMS and SHAM TMS conditions, using an intensity three times (in four subjects four times) the individual's sensory perception threshold (on average, 25.6 ± 7.5 mA), with a pulse width of 50 μs. ES was delivered exactly concurrently with the TMS trigger. This procedure was employed in order to saturate the PEPs in both the ACTIVE and SHAM TMS conditions and, therefore, equalize them in both conditions (Gordon et al., 2021). This should hold true even when considering that the ACTIVE TMS condition also involves somatosensory input from the TMS pulse, which will become negligible in the presence of the high-intensity saturating somatosensory input provided by ES. Therefore, we argued that it is then possible to subtract the resulting SHAM TMS-EEG response (only PEPs) from the ACTIVE TMS-EEG response (containing both PEPs and TEPs), thus obtaining the brain responses specifically caused by direct cortical activation (TEPs). The sensory perception reported by the subjects was highly comparable between the ACTIVE and SHAM TMS conditions (Fig. 2).

EEG data processing

Offline data analysis was performed using the FieldTrip open-source toolbox (Oostenveld et al., 2011). The resting-state EEG signal was first segmented in 3 s epochs. Spectral power was estimated using the Irregular Resampling Auto-Spectral Analysis (IRASA) method as implemented by the FieldTrip toolbox, and the signal-to-noise ratio was then computed by subtracting the fractal (aperiodic) component from the full spectrum (Donoghue et al., 2020).

To analyse time-domain EEG responses to TMS (TEPs), the signal from each measurement was segmented into epochs aligned to the TMS pulse (−1000 to 1500 ms) in both the ACTIVE and SHAM conditions, and then baseline corrected (−1000 to −50 ms). Both TMS and direct scalp ES are prone to produce a marked decay artefact that can affect the EEG signal from the first few milliseconds up to hundreds of milliseconds. To remove this artefact, we subtracted the best fit of an exponential function from each trial and channel (Conde et al., 2019; Rogasch et al., 2017). For this purpose, we used the 'fit' function from MATLAB to fit the one-term exponential model ($a \times \exp(b \times x)$) over every epoch during the time window 15–500 ms after the TMS pulse. With the prior knowledge that the decay artefact mostly affects early time points, a weighting factor for the exponential model was used, which incorporated a linearly spaced array of 100 to 1 over the course of the fitting time. To prevent the slow
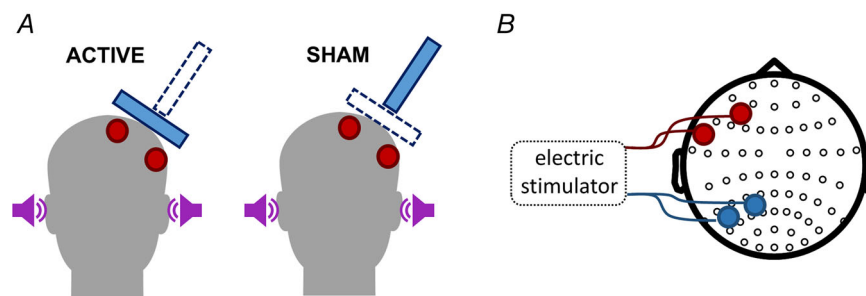

Figure 1. Stimulation set-up
A, representation of the ACTIVE and SHAM TMS set-up, showing delivery of masking noise (purple sound icons) and electrical stimulation of the scalp (red circles) in both stimulation conditions. The difference is with respect to the TMS coil, as ACTIVE TMS involved discharging the coil tangential to the scalp, whereas SHAM TMS involved discharging the coil tilted 90° with respect to the scalp (blue rectangles). *B*, topographical plot illustrating the EEG electrodes over the scalp and the relative position of electrodes for electrical stimulation: two electrodes of the same polarity at FFT9h and AFF5h (red circles), and two electrodes of the opposite polarity at CPP3h and TPP7h (blue circles), connected to the electrical stimulator device. Polarity switched after each pulse. [Colour figure can be viewed at wileyonlinelibrary.com]

waves of artefacts from contaminating the decay model, the exponential fit was obtained from detrended data, in which a fifth degree polynomial was subtracted from every epoch. Following the exponential decay subtraction, the time window between −5 and 15 ms around the TMS pulse, still containing the high-amplitude TMS artefact, was removed and cubic interpolated. EEG data were then downsampled to 1 kHz. Trials were inspected visually, and epochs and channels with excessive noise were excluded, as were trials containing MEPs in the EMG of the right FDI or APB. The average percentage of trials excluded per subject was 19.6% (SD ± 11.2%), with 4.6% due to the presence of MEP (SD ± 5.1%), while the number of channels excluded was on average 5.5 (SD ± 2.1). Further artefacts were removed with independent component analysis (ICA), including artefacts related to muscle activity, eye movement and blinks (Rogasch et al., 2014), using the FastICA algorithm implemented in FieldTrip (Oostenveld et al., 2011). Excluded channels were spline-interpolated. Channels exclusion and interpolation, as well as ICA, were performed separately for each intervention (diazepam, placebo) of a given individual, but combining the data of the measurements before and after drug intake. The TEP signal was finally filtered with a 45 Hz low-pass filter. These procedures yielded the EEG response from the ACTIVE and SHAM conditions. To obtain the ACTIVE minus SHAM condition (i.e. the TMS-EEG response without the PEP) we subtracted the SHAM from the ACTIVE EEG responses. This was done at the individual level, separately for the measurements of each drug intervention (i.e. diazepam *vs.* placebo) and time (i.e. pre- *vs.* post-drug intake).

For the processing of TMS-induced oscillations, time–frequency representations (TFRs) of TMS-related changes in oscillatory power were calculated both trial-by-trial and for the average of all trials. The TFR of the average of all trials was then subtracted from the TFR of each trial, thus removing the evoked oscillatory response and obtaining only the induced oscillatory response (Pellicciari et al., 2017). TFR was calculated using a Morlet wavelet decomposition on single trials, with frequency-dependent width (wavelet width of 2.6 cycles at 4 Hz, adding 0.2 cycles for each 1 Hz). This was followed by standardizing the TFR, by calculating the z-value in each frequency band using the pre- and post-stimulus epoch (Grandchamp & Delorme, 2011), and baseline correction (−500 to −50 ms). The procedure was performed trial-by-trial, which entailed separation of the pre- and post-drug conditions. This was relevant in order to standardize the baseline of all measurements in case of a change in the overall oscillatory activity after an intervention.

EEG activity from statistically significant results was localized into the source space. Individual cortical surfaces and dipole arrays were obtained from the individual's MRI, segmented and meshed using the FieldTrip toolbox (Oostenveld et al., 2011), with a forward model for EEG using a customized pipeline, taking into account the positions of the EEG electrodes relative to individual head anatomy (Stenroos & Nummenmaa, 2016; Stenroos & Sarvas, 2012). Source reconstruction was then obtained on the whole cortical surface using the L2-minimum-norm estimate (Hamalainen & Ilmoniemi, 1994). For the TEPs, the final result was obtained by
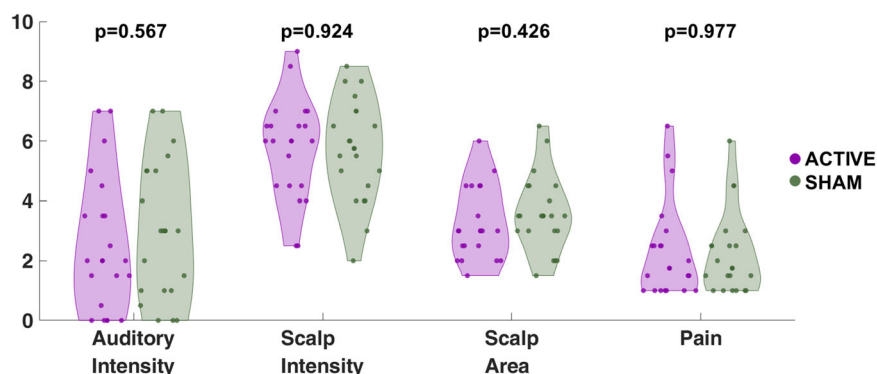
Figure 2. Sensorial perception of the ACTIVE *versus* SHAM TMS conditions
Results from visual analogue scale testing for subjective perception of sensory intensity. Four sensory modalities caused by the ACTIVE *vs.* SHAM TMS conditions were tested: intensity of auditory input, intensity of somatosensory (scalp) input, size of the scalp area where the somatosensory input was perceived, and pain/discomfort caused by the somatosensory input. Reported responses could range from 0 (no perceived sensory modality) to 10 (highest intensity possible). Each point corresponds to the response from one individual subject. Comparisons between the ACTIVE *vs.* SHAM TMS results were performed with Wilcoxon's signed-rank test for non-normal distributions, and resulting *P*-values are displayed above each sensory modality. The tests were performed in the experiment described in Gordon et al. (2021). In the current analysis, only the 20 subjects were included that proceeded to the pharmacological interventions experiment, described in the present report. [Colour figure can be viewed at wileyonlinelibrary.com]

z-transforming the signal of each trial with respect to the mean and standard deviation of the baseline (−500 to −50 ms). For induced oscillations, the EEG signal was first projected to the source space, followed by the TFR calculation, as described above. For the purpose of plotting the final results, data attributed to each individual dipole was pooled and warped into a common MNI space for creating a group average across all subjects.

Statistical analysis

All statistical analyses were performed on the MATLAB platform (R2018b, The Mathworks, USA). Cluster-based permutation *t* tests were implemented using the FieldTrip toolbox, using 1000 permutations per test (Oostenveld et al., 2011). We compared all EEG-related measures, described above, post-intervention *vs.* pre-intervention, separately for the diazepam and placebo conditions.

The resting-state EEG data were *a priori* divided into frequency bands of interest (FOI): theta (4–7 Hz), alpha (8–12 Hz), low beta (13–20 Hz), high beta (21–29 Hz) and gamma (30–45 Hz). The signal-to-noise ratio from each FOI was then averaged in each channel and submitted to cluster-based *t* tests for the post- *vs.* pre-intervention comparisons, yielding the significant channel clusters. Because of the multiple testing imposed by the five FOIs, the threshold of statistical significance was Bonferroni-adjusted to $P < 0.01$.

Regarding the TEP analysis, instead of predetermining a set of time windows of interest after the TMS pulse where differences are expected to occur, we relied on the cluster-based *t*-statistics to determine any time window (between 20 and 500 ms after the TMS) that contained significantly different EEG responses. We first set the cluster-based *t* tests to include all the channels and time samples, in order to estimate the time windows where the EEG responses were significantly different post- *vs.* pre-intervention. The EEG responses were then averaged within these significant time windows and compared by only including the channels in the cluster calculation, yielding the significant channel clusters. The significance threshold was set to $P < 0.05$. Analyses were performed by comparing the post- *vs.* pre-intervention data separately in the ACTIVE and SHAM TMS conditions. Finally, the post- *vs.* pre-intervention measurements were compared after subtracting the SHAM TMS response from the ACTIVE TMS response.

Statistical analysis of the TMS-induced oscillations followed the same procedure as for the TEPs, but first the data were divided into the same five FOIs as the resting-state EEG data. Therefore, the threshold for statistical significance was adjusted to $P < 0.01$.

Results

Drug effects on resting-state EEG

Diazepam led to significant changes of the resting-state EEG power spectrum (Fig. 3*A*). The cluster-based *t*-statistics revealed a decrease in alpha power following diazepam intake, observed in a cluster that comprised most of the electrodes. Diazepam also led to an increase in beta power, with low-beta increase detected over the entire scalp, whereas the high-beta increase was limited to the midline regions (Fig. 3 *C–D*). Cluster-based *t*-statistics did not yield any significant cluster when comparing the power spectra post- *vs.* pre-placebo intervention in any frequency band of interest (Fig. 3*B*).

Drug effects on TEPs

Figure 4 shows the butterfly time-course plots of TMS-EEG responses to both drug interventions over all electrodes. As expected, placebo intake did not result in any observable change in either ACTIVE or SHAM TMS (Fig. 4*A*). In contrast, diazepam led to evident changes of the TMS-EEG response, either largely indiscriminately in the ACTIVE and SHAM responses in the period 100−150 ms, or largely selectively in the ACTIVE TMS minus SHAM response in the period around 60 ms (Fig. 4*B*).

The cluster-based *t*-statistics on the post- *vs.* pre-diazepam SHAM responses revealed a highly significant decrease of the fronto-central negative potential peaking at around 120 ms, and a decrease in the posterior positive potential at around 250 ms (Fig. 5). Given that the SHAM condition involved only multisensory input but not TMS of the brain, these results indicate a specific effect of diazepam on PEPs, consisting of an amplitude reduction of late (>85 ms) TMS-EEG potentials, including an almost complete suppression of the N100 (Figs 5 and 6*A*).

The cluster-based *t*-statistics on the post- *vs.* pre-diazepam ACTIVE TMS late responses (>80 ms) are similar to those in the SHAM condition (Figs 5 and 6*B*). This is expected, since both conditions involve saturated multisensory input. One difference is a cluster specific to the ACTIVE TMS condition (i.e. not observed in the SHAM condition) comprising left frontal electrodes with increased negativity of the potential around 40–65 ms (P60) (Fig. 5). Source space projection of the signal indicated that this response was located in the stimulated region, around the left M1, extending to frontal regions of the ipsilateral cortex (Fig. 6*B*).

Finally, the post- *vs.* pre-diazepam comparison of the ACTIVE TMS minus SHAM response revealed three significant clusters. The first cluster showed increased negativity of the P60 over left frontal electrodes. Just as for

P. C. Gordon and others

the ACTIVE TMS condition, the source space projection indicated that this response is located in the area of the stimulated left M1 and respective frontal region (Fig. 6*C*), further suggesting that this modulation is specific to a response caused by TMS rather than by sensory input. The second cluster revealed increased negativity around 140–155 ms (P150) over the left sensorimotor cortex, and the third cluster demonstrated increased negativity at 210−250 ms over bilateral prefrontal cortices (Fig. 6*C*).

Cluster-based *t*-statistics did not yield any significant cluster in the placebo intervention in either SHAM, ACTIVE TMS or ACTIVE TMS minus SHAM conditions.

These results suggest that diazepam has significant effects both on TEPs (represented by the subtraction ACTIVE TMS − SHAM) and on PEPs (represented by indiscriminate effects in the ACTIVE TMS and SHAM conditions). The effects of diazepam on TEPs were also partially represented, as expected, in the ACTIVE TMS

signals, but to a lesser or even lacking extent (P150), probably due to the superimposition of diazepam effects on the PEPs at latencies >85 ms.

Finally, although the ACTIVE TMS − SHAM signal showed a clear positive deflection over the stimulated sensorimotor cortex at around 30 ms (P30), this TEP was not significantly modulated by diazepam (Fig. 6 *B* and *C*).

Drug effects on TMS-induced oscillations

The post- *vs.* pre-diazepam comparison revealed no significant difference in the induced oscillations in the SHAM condition (Fig. 7). In the ACTIVE TMS condition, diazepam led to a significant decrease in TMS-induced oscillations in the low- and high-beta frequency bands in the first 200 ms (Fig. 7 *A*–*B*). In the ACTIVE TMS minus SHAM response, a significant cluster was found only in
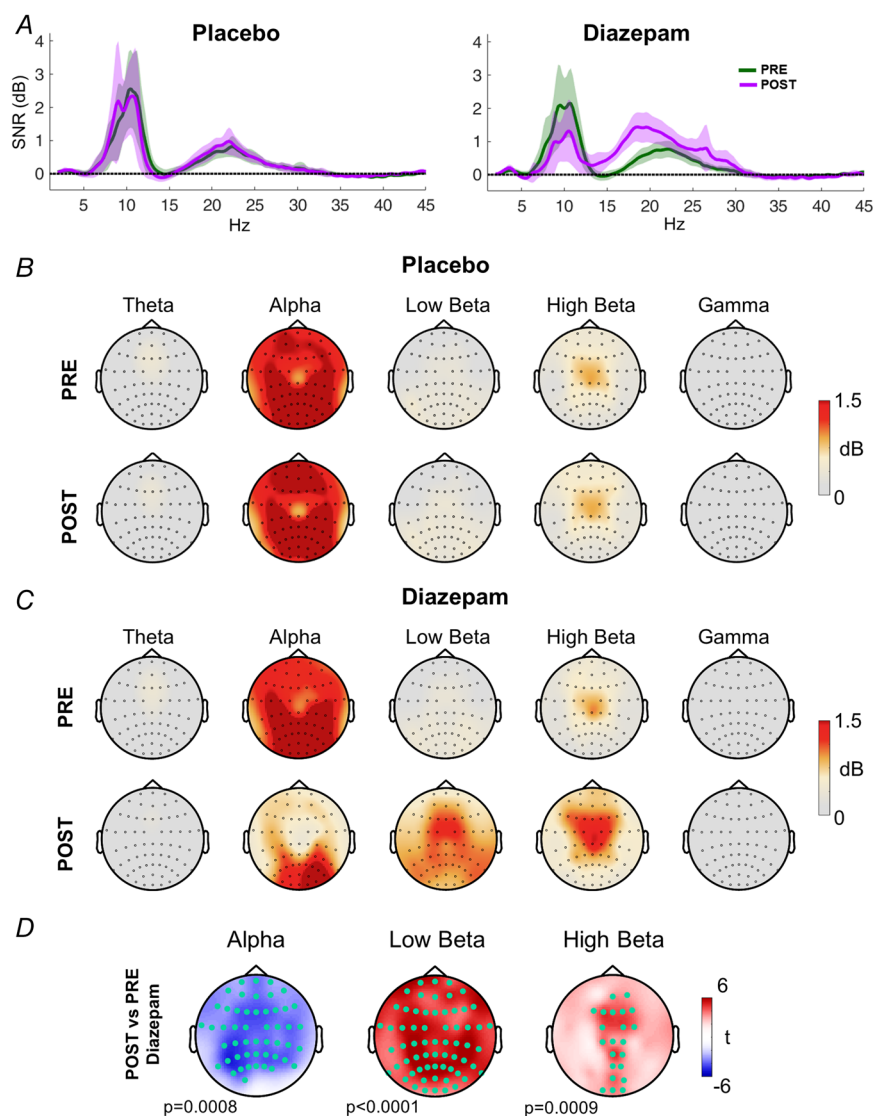
**Figure 3. Resting-state EEG analyses post vs. pre drug**
A, power spectra of resting-state EEG signal (shades correspond to 1 SD), obtained before (PRE, green line) and after (POST, purple line) intake of placebo (left) or diazepam (right). *B*, scalp distribution of the signal-to-noise ratio (SNR) of each frequency band of interest: theta (4–7 Hz), alpha (8–12 Hz), low beta (13–20 Hz), high beta (21–29 Hz) and gamma (30–45 Hz). Data shown correspond to the PRE (top row) and POST measurements (bottom row) of the placebo intervention. Cluster-based *t*-statistics did not yield any significant cluster when comparing the power spectra post- *vs.* pre-placebo intervention in any frequency band of interest. *C*, scalp distribution of the signal-to-noise ratio of each frequency band of interest, as in *B*, of the PRE and POST measurements of the diazepam intervention. *D*, topographical plots of the cluster-based *t*-statistics comparing the power spectra of resting-state EEG post- *vs.* pre-diazepam, highlighting the electrodes (cyan dots) that comprised the statistically significant clusters. Red and blue colours indicate increase and decrease in power, respectively. [Colour figure can be viewed at wileyonlinelibrary.com]

the low-beta frequency band in left post-central electrodes (Fig. 7 *A–B*). The analysis in source space demonstrated that TMS leads to an increased beta response in the first 200 ms after the stimulus in the stimulated sensorimotor cortical region (Fig. 7*C*), which was absent in the SHAM condition and, therefore, cannot be explained by a modulatory effect of diazepam on the responses to multisensory input.
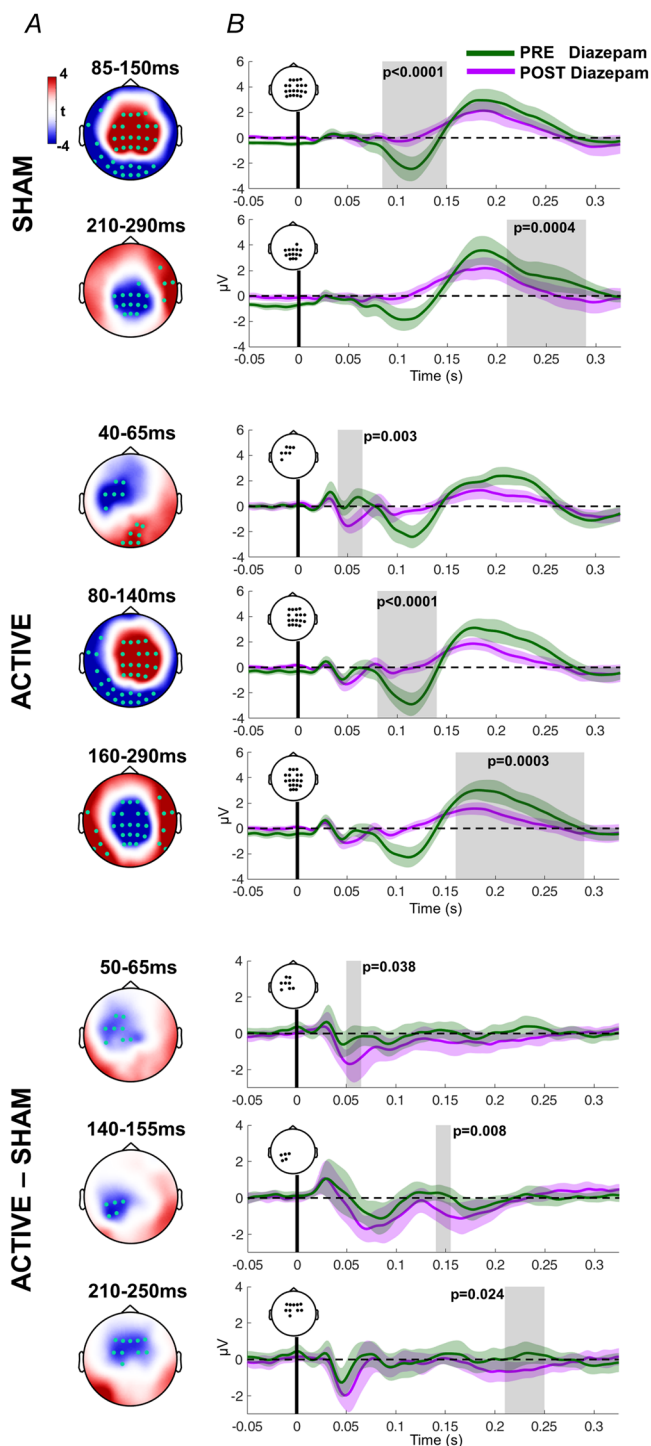
Discussion

The present observations significantly extend the results from previous studies. In agreement with previous data, diazepam led to modulation of TMS-EEG responses at both early (<80 ms) and later latencies (Premoli et al., 2014). This was observed in the responses to ACTIVE TMS, and persisted after subtraction of the SHAM
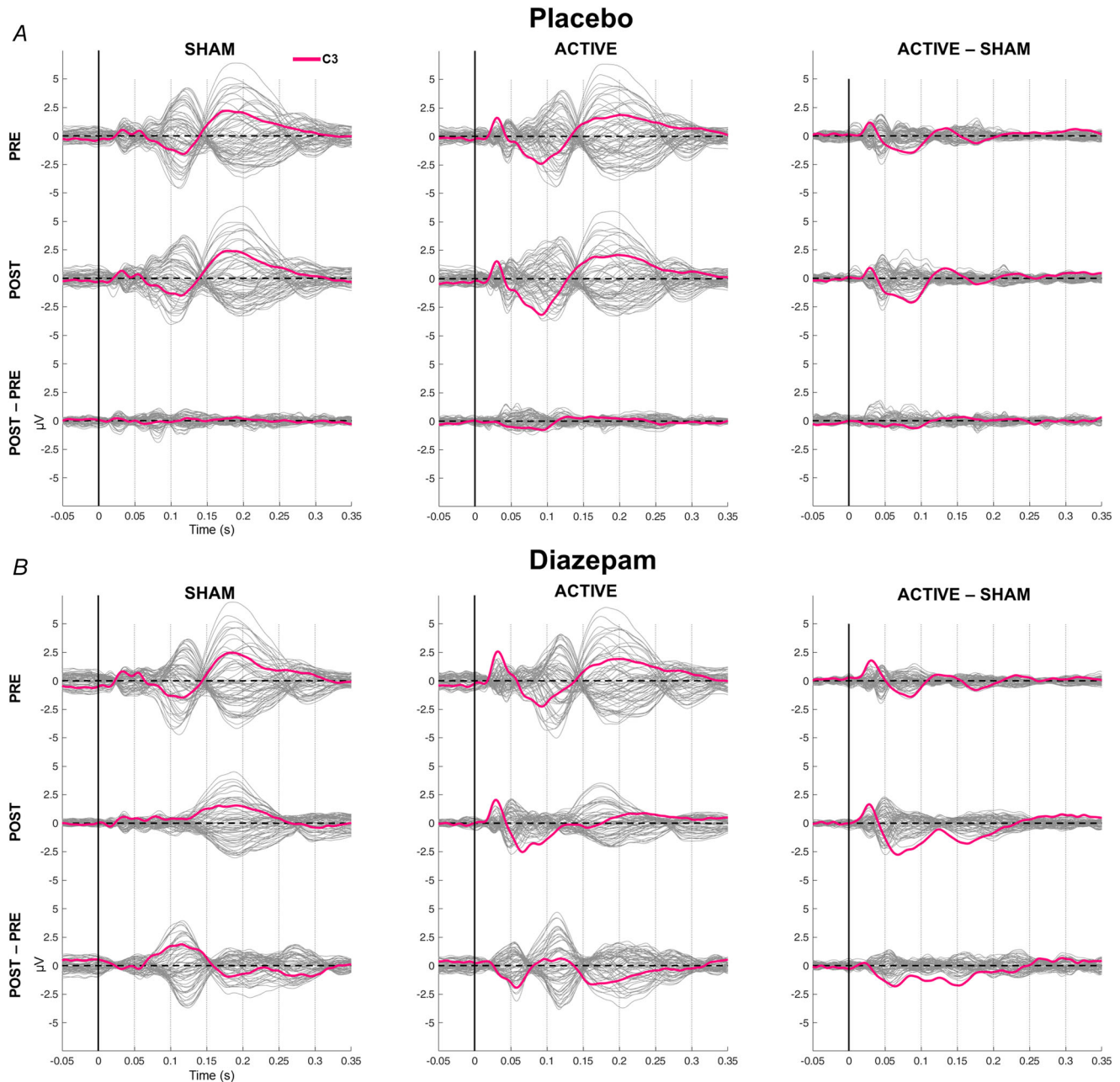
Figure 4. ACTIVE vs. SHAM TMS-EEG responses post vs. pre drug
Time course of the TMS-EEG responses to each intervention (*A*, placebo; *B*, diazepam), time (pre- and post-intervention) and stimulation condition (SHAM, ACTIVE TMS, ACTIVE TMS minus SHAM), with stimulation time marked with a black horizontal line at time = 0. Plots display averages across all subjects (*n* = 20), each grey line represents the signal from one EEG electrode. Red lines indicate the signals from the C3 electrode. [Colour figure can be viewed at wileyonlinelibrary.com]

significance of respective clusters is displayed as *P*-value. Results refer to the POST- *vs*. PRE-diazepam measurements (purple and green, respectively). Shades correspond to 1 SD. Grey areas indicate the time windows of the significant clusters. [Colour figure can be viewed at wileyonlinelibrary.com]

Figure 5. ACTIVE vs. SHAM TMS-EEG responses post vs. pre diazepam

A, topographical plots of the cluster-based *t*-statistics comparing TMS-EEG responses POST- and PRE-diazepam highlighting electrodes that comprised the significant clusters (cyan dots). Results are divided in responses elicited by SHAM TMS (top), ACTIVE TMS (middle) and ACTIVE TMS minus SHAM (bottom). *B*, time course of the EEG response following stimulation (indicated by black bars at time 0 s), averaged across all subjects (*n* = 20) and the electrodes that composed the significant clusters displayed in the respective top-left inset (black dots in the topographical model). Statistical
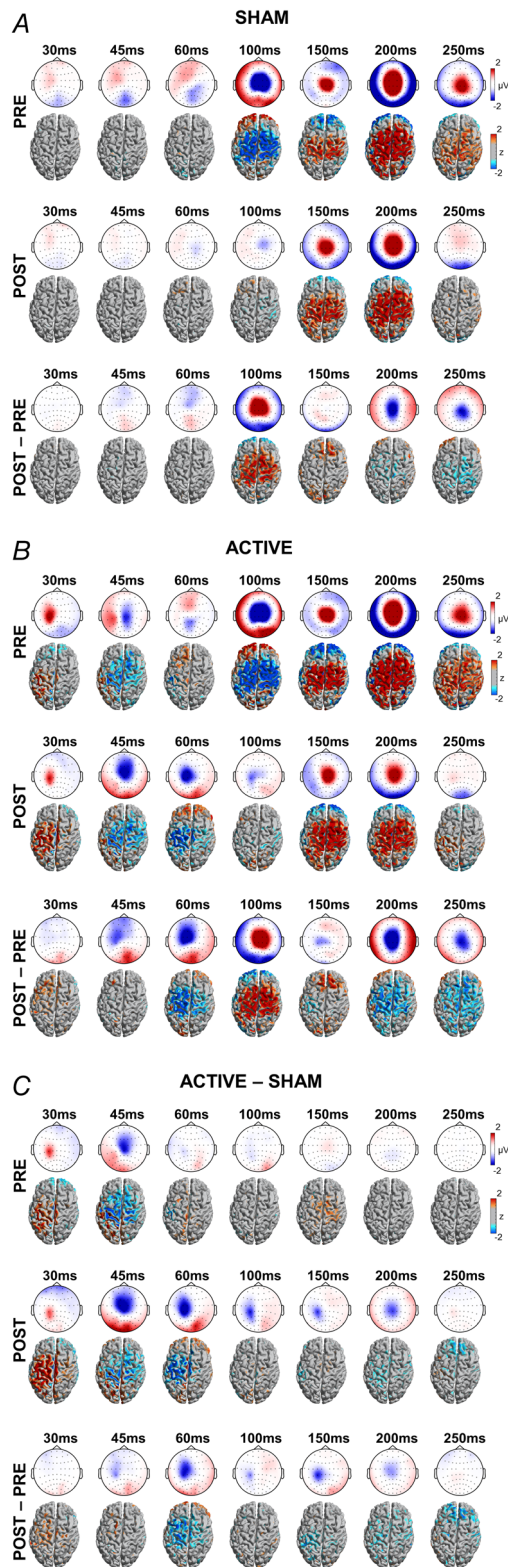
response from the ACTIVE TMS response, strongly suggesting a modulatory effect of diazepam on EEG responses to direct cortical activation by TMS. Another result matching previous findings was the substantial amplitude reduction of the negative TMS-EEG deflection around 100 ms (N100). However, this diazepam effect was observed in the EEG responses elicited by both ACTIVE TMS and SHAM but vanished after subtracting the SHAM from the ACTIVE TMS response. This provides evidence that the diazepam effect on the N100 amplitude was caused by PEP rather than TEP modulation. These findings have critical consequences for the implementation and interpretation of TMS-EEG experiments.

The role of PEPs in TMS-EEG

EEG responses to sensory input have long been observed in TMS-EEG experiments (Ilmoniemi & Kicic, 2010; Nikouline et al., 1999), characterized as a negative cortical deflection peaking at around 100−120 ms, predominantly expressed in the fronto-central midline scalp regions, followed by a positive deflection at around 180−200 ms in posterior regions (Ahn & Frohlich, 2021; Biabani et al., 2019; Ilmoniemi & Kicic, 2010). This pattern fits the profile of EEG responses to perceptual inputs, which are classified as event-related potentials (ERPs) (Boutros et al., 2011; Courchesne et al., 1975; Friedman et al., 2001; Lijffijt et al., 2009; Singhal et al., 2002). These ERPs, often referred to as the N100–P200 complex, can be elicited by a variety of stimuli, suggesting that the response is largely independent of the sensory modality and represents supramodal processing of perceptual inputs (Downar et al., 2002; Kenemans, 2015; Mouraux & Iannetti, 2009; Singhal et al., 2002). Multiple cortical areas contribute to this response, including superior temporal cortex, anterior and posterior cingulum, inferior parietal cortex, and broad regions of the frontal cortex, as determined by both intracranial recordings (Boutros et al., 2011) and functional MRI (Kiehl et al., 2005; Strobel et al., 2008). These ERPs have been interpreted as responses generated by cortical and subcortical networks involved in the modulation of attention and responses to unexpected or salient perceptual events (for review, Wessel & Aron, 2017).

Since TMS-EEG aims at probing focal cortical responses to direct activation by TMS, the overlapping of

row), post-diazepam (middle row) and post-diazepam minus pre-diazepam (bottom row). Cortical model plots below the topographical plots show source projections of the corresponding signals, displayed as *z*-scores. [Colour figure can be viewed at wileyonlinelibrary.com]

PEPs in the response signal represents a relevant limitation of the method. This led to attempts to control for the presence of PEPs, often by employing a control condition that recreates the same sensory inputs as the ACTIVE TMS, in the form of a SHAM TMS condition. The response signal from this sham condition can then be subtracted from the ACTIVE TMS-EEG signal, as we are proposing here. Alternative methods for removing PEP components from the TMS-EEG response include independent components analysis (Ross, Ozdemir et al., 2022) and signal-space projection (Biabani et al., 2019). Other approaches involve analysing signal similarities between TMS-EEG responses elicited by ACTIVE TMS *versus* SHAM TMS using correlation analysis (Conde et al., 2019) and cosine similarity-based analysis (Freedberg et al., 2020). These latter approaches confirmed the notion that TMS-EEG responses <80 ms after the TMS pulse are mostly free from overlapping PEPs, although they were not designed to remove PEPs from the TMS-EEG signal. Moreover, it is important to note that all methods that have attempted to remove PEPs assumed independence between PEPs and TEPs (Biabani et al., 2019). Also, they require information on the signal components that need to be removed from the data of interest, typically obtained with a SHAM TMS condition. Ideally, SHAM TMS should deliver the same multisensory inputs as ACTIVE TMS, thereby allowing the thorough removal of the PEP components from the EEG response elicited by ACTIVE TMS (Biabani et al., 2019; Casali et al., 2010; Du et al., 2017; Gordon et al., 2018; Gordon et al., 2021; Herring et al., 2015).

The role of GABAAR-mediated neurotransmission in PEPs

Several reports have consistently described ERP amplitude reductions by benzodiazepines (Lindhardt et al., 2001; Rockstroh et al., 1991; van Leeuwen et al., 1995), as well as modulation of cortical oscillatory activity (Hall et al., 2010; Saletu et al., 1994). Both ERPs and EEG oscillations are understood to result from complex cortical and sub-cortical mechanisms, including cortico-thalamic circuits involved in the generation of low-frequency oscillations, in which populations of GABAergic neurons have an integral role (Huguenard & McCormick, 2007; Ketz et al., 2015).

Figure 6. Topographical plots of ACTIVE vs. SHAM TMS-EEG responses post vs. pre diazepam
Topographical plots of the scalp distribution of the TMS-EEG response amplitudes following SHAM TMS (*A*), ACTIVE TMS (*B*) and ACTIVE TMS minus SHAM (*C*), at different time points, averaged across all subjects (*n* = 20). Data correspond to pre-diazepam (top

Increased GABAAergic tone directly affects neuro-transmission in cortico-thalamic circuits, resulting in oscillatory power shifts that can be detected as increased power in the beta band in the resting-state EEG (Fig. 3*A*) and magnetoencephalography recordings (Hall et al., 2010). Several complementary functions have been attributed to cortical beta oscillations. Increased beta power has been associated with an enhanced cortical inhibitory state, which prevents the arrival of incoming information, a necessary mechanism for the maintenance of items in working memory, or the continuous execution of motor planning (Engel & Fries, 2010; Miller et al., 2018). Modulation of beta oscillations and the occurrence of bursts in the beta frequency have also been observed as a response to and processing of sensory cues and motor signals (Schmidt et al., 2019; Zavala et al., 2018). By promoting a state of increased GABAAergic tone and beta activity, diazepam leads to a deficient perception of and response to salient stimuli. This is reflected in the suppression of ERP (N100) and oscillatory responses, which have also been correlated with the behavioural and cognitive deficits caused by positive allosteric modulators of GABAARs (Lozano-Soldevilla et al., 2014).

Therefore, the observed effect of diazepam on the N100 may simply correspond to modulation of the N100–P200 complex, which we had mistakenly inter-preted as GABAAergic modulation of the TMS-EEG response to direct cortical activation in previous studies (Premoli et al., 2014). Further, this novel insight may question to what extent interpretation of results from other TMS-EEG studies remain valid. For instance, TMS-EEG studies have shown an abnormally low N100 amplitude in neuropsychiatric disorders such as ADHD, schizophrenia and substance abuse (Bruckmann et al., 2012; Loheswaran et al., 2018; Noda et al., 2018). All these conditions have also been associated with
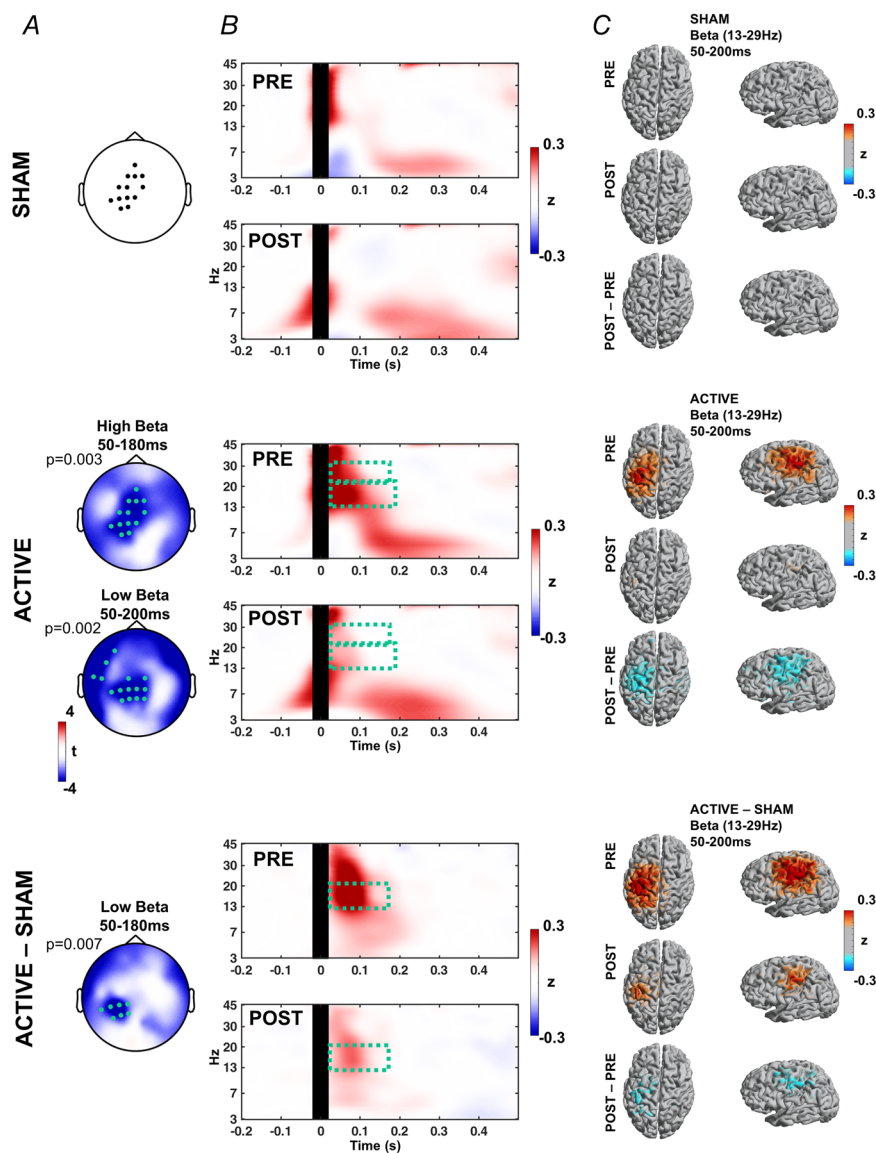
Figure 7. ACTIVE vs. SHAM TMS-induced oscillations post vs. pre diazepam
A, topographical plots of cluster-based *t*-statistics of induced oscillations post- *vs.* pre-diazepam intake, highlighting electrodes (cyan dots) that comprised the statistically significant clusters (note that no significant cluster was found in the SHAM condition). *P*-values of the respective clusters are indicated. Results are divided in induced oscillations elicited by SHAM (top), ACTIVE TMS (middle) and ACTIVE TMS minus SHAM (bottom). *B*, time–frequency plots displaying the subtraction post- minus pre-diazepam intake. Data averaged across all subjects (*n* = 20) and channels comprising the respective significant clusters in (*A*). For the SHAM condition, the same electrodes were used that comprised the significant cluster in the high-beta band in the ACTIVE TMS condition. Time–frequency regions of the significant clusters are outlined with cyan dotted boxes. *C*, cortical model plots show source projections of the induced oscillations post- minus pre-diazepam intake within the specified frequency and time windows. [Colour figure can be viewed at wileyonlinelibrary.com]

pathologically low sensory ERP amplitudes (Cheng et al., 2016; Rangaswamy & Porjesz, 2014; Rosburg, 2018). Likewise, consistent modulation of the N100 potential has been described following theta-burst stimulation to the prefrontal cortex (Che et al., 2019; Chung et al., 2017; Chung et al., 2019), which, given the role of prefrontal regions in the generation of ERPs, might simply indicate modulation of PEP rather than TEP amplitudes.

However, our results do not automatically imply that other previous TMS-EEG studies are to be considered invalid. In particular, TMS-EEG responses at latencies <80 ms after the TMS pulse are at low risk for being contaminated with PEPs (Ahn & Frohlich, 2021; Conde et al., 2019) and, therefore, likely represent genuine focal cortical responses to direct activation by TMS. Nevertheless, the present findings reinforce the argument that the use of proper control for PEPs is crucial in TMS-EEG experiments, to allow removal of PEPs from the TMS-EEG signal and reveal responses specifically attributed to direct cortical activation by TMS, including responses that might otherwise have been concealed by PEPs. This is the case for the positive deflection observed in the stimulated sensorimotor cortex around 150 ms after the stimulus. In a recent report (Gordon et al., 2021), we demonstrated the existence of this response to TMS of M1. However, the P150 became visible only in the ACTIVE TMS minus SHAM response. Here we show, in addition, that the P150 is suppressed by diazepam, and again, this effect could be demonstrated only in the ACTIVE TMS minus SHAM response (Figs 5 and 6*C*).

Revisiting the role of GABAAR-mediated neurotransmission in TMS-EEG

The earliest TMS-EEG response was a clearly identifiable positive deflection around 30 ms after the TMS pulse, at the stimulation site, which has been described by several previous reports (Bonato et al., 2006; Komssi et al., 2004; Lioumis et al., 2009; Paus et al., 2001). However, this deflection remained unaffected by the intake of diazepam (Fig. 6*B*). This reproduces the observations from our previous study, suggesting that this component is insensitive to GABAAR modulation (Premoli et al., 2014), while it may be suppressed by blockers of voltage-gated sodium channels, such as carbamazepine (Darmani et al., 2019). Although the origin of this component is not well understood, its amplitude is affected by the direction of the induced electrical field in the sensorimotor cortex, and some studies demonstrated a correlation with MEP amplitude, although other reports could not replicate this finding (Ahn & Frohlich, 2021; Bonato et al., 2006; Maki & Ilmoniemi, 2010).

We showed previously that the anti-glutamatergic drug perampanel (antagonist at the α-amino-3-hydroxy-5-methyl-4-isoxazole propionic acid receptor) also caused suppression of the P60 (Belardinelli et al., 2021). In combination with the diazepam effect of the present study, these results suggest that the P60 amplitude reflects an excitation/inhibition balance. Shifts towards less excitation/more inhibition result in P60 amplitude depression.

Finally, the time window and location of the P150 are similar to those of the low beta-band oscillatory response, which is also a specific response to TMS of M1 independent of sensory inputs (Gordon et al., 2021; Hannah et al., 2022). Moreover, both of these responses are suppressed by diazepam (Fig. 7) (Premoli, Bergmann et al., 2017).

Comparison with the previous pharmaco-TMS-EEG study by Premoli et al. (2014)

There are relevant methodological differences between the present and the previous pharmaco-TMS-EEG study (Premoli et al., 2014), which are most likely responsible for differences in the findings between the two studies. Firstly, we applied here subthreshold TMS intensity, whereas the previous study (Premoli et al., 2014) used TMS pulses at threshold intensity. TMS of motor cortex at suprathreshold intensities results in different TMS-EEG responses compared with subthreshold TMS (Gordon et al., 2018; Romero et al., 2019). In particular, suprathreshold stimulation elicits a prominent negative deflection in bilateral frontal and contralateral sensorimotor cortex (N45) (Biabani et al., 2019; Bonato et al., 2006; Gordon et al., 2018), compared with a more localized and lower amplitude potential elicited by subthreshold TMS (Fig. 6*B*) (Biabani et al., 2019; Bonato et al., 2006; Gordon et al., 2018). Given the capacity of suprathreshold TMS to effectively depolarize pyramidal neurons in deeper cortical layers (Romero et al., 2019), TMS pulses are likely to result in the propagation of action potentials from the target region, causing the activation of connected distant cortical areas, such as the contralateral sensorimotor cortex. Premoli et al. (2014) concluded that diazepam acted in modulating this propagation, resulting in the observed change in the N45 contralateral to the stimulation site (Premoli et al., 2014). This effect, however, was not observed in the present study, most likely because of the use of subthreshold stimulation intensity.

Moreover, suprathreshold TMS of M1 elicits negative deflections between 100 and 200 ms centred at the site of stimulation (Biabani et al., 2019; Gordon et al., 2018). Conversely, subthreshold TMS of M1 elicits a positive deflection in the stimulated sensorimotor region around 150 ms after the stimulus, which is independent of sensory input, as demonstrated here (Fig. 5) and in previous reports (Gordon et al., 2021; Hannah et al., 2022). In addition, suprathreshold TMS pulses are accompanied by another peripherally evoked response, the re-afferent

feedback resulting from the MEP-related muscle twitch (Fecchio et al., 2017; Petrichella et al., 2017). This would constitute an additional confounding factor to the TMS-EEG analysis, which explains our present choice of using a subthreshold stimulation intensity. Another crucial difference is that the previous study lacked a SHAM condition (Premoli et al., 2014). This incapacitated the previous study from disentangling TEPs from PEPs, a major limitation for interpretation of TMS-EEG responses at latencies >80 ms.

Limitations

As evident from the reported sensory input (Fig. 2), a considerable proportion of subjects could identify the TMS 'click' sound despite the masking noise. This failure to completely suppress the TMS sensory input occurs as some subjects and stimulation conditions require high TMS intensities, which produce auditory inputs that surpass the masking noise (Conde et al., 2019; Gassmann et al., 2022). TMS-related auditory inputs, however, have been successfully controlled with the introduction of a sham coil that produced the same 'click' sound as the active coil. Nevertheless, the design of effective masking noise for specific TMS setups has been facilitated with the recent development of open-source toolboxes for this purpose (Russo et al., 2022), which can create a device-specific masking noise capable of suppressing the TMS 'click' even at lower sound intensities, thus dispensing with the need for a sham control for auditory inputs.

Proper control for somatosensory inputs, however, are still necessary, especially when applying TMS to sensitive regions of the scalp or using high TMS intensities. This is evident by the detection of PEPs in TMS-EEG signal even after thorough control for auditory sources (Ross, Sarkar et al., 2022). In the present experiment, we controlled for somatosensory inputs by means of an optimized sham procedure, which is based on the assumption that the TEPs and PEPs are linearly superimposed. However, this would not be true in the case of an interaction effect between TEPs and PEPs, which would invalidate the procedure. This motivated us to design a further experiment to test this hypothesis, recently published (Gordon et al., 2023). In that experiment, we observed no evidence of TEP modulation by sensory inputs, which remained stable regardless of the concomitant PEPs. Therefore, there is currently no evidence that sensory responses interact with the cortical responses from TMS measured by EEG, further supporting the validity of the PEP subtraction from TEPs in TMS-EEG studies.

The use of high-intensity ES may still have other limitations, such as subject discomfort and increased risk of electrical artefacts in the EEG. Therefore, despite the efficacy of the present optimized SHAM procedure in removing the PEPs from the TMS-EEG signal, there is room for improvement. A possible solution could be to determine the amplitude of the PEPs elicited by TMS, and titrate ES intensity to elicit the same response, thus eliminating the need to apply ES in the ACTIVE TMS condition (Gordon et al., 2023). Moreover, other procedures to remove PEPs from the TMS-EEG response might be more reliable than the plain signal subtraction, such as the use of ICA and signal-space projection (Biabani et al., 2019; Ross, Ozdemir et al., 2022), although this will have to be further tested in future experiments.

A final issue concerns the concept of 'true' TEPs. In the present study we successfully extracted the EEG response from TMS by removing the spurious responses to sensory input. Nevertheless, the characteristics of these responses, both in time and cortical distribution, are considerably variable and dependent on several factors, including TMS intensity, exact cortical target, brain state during the stimulation and inter-individual variability. Despite standardization procedures to account for most of these factors, the inter-individual variability is still an issue that has not been systematically tackled, and which we could not address in the present study due to its limited sample size. In addition to properly controlling for PEPs, future TMS-EEG studies would benefit from accessing the role of inter-individual variability in the EEG responses to cortical TMS.

Conclusions

We demonstrated that diazepam, a positive allosteric modulator of GABAARs, specifically suppressed certain components (P60, P150, induced oscillations in the low-beta frequency band) of the ACTIVE TMS minus SHAM response, and indiscriminately suppressed the N100 component of the ACTIVE TMS and SHAM responses. These findings provide compelling evidence that the optimized SHAM condition can be used to clean PEPs from TEPs by subtraction of the SHAM from the ACTIVE TMS response. This advancement of knowledge of the physiology of TMS-EEG responses will facilitate their utilization in further physiological and clinical investigations.

References

Ahn, S., & Frohlich, F. (2021). Pinging the brain with transcranial magnetic stimulation reveals cortical reactivity in time and space. *Brain Stimulation*, **14**(2), 304–315.

Belardinelli, P., Konig, F., Liang, C., Premoli, I., Desideri, D., Muller-Dahlhaus, F., Gordon, P. C., Zipser, C., Zrenner, C., & Ziemann, U. (2021). TMS-EEG signatures of glutamatergic neurotransmission in human cortex. *Scientific Reports*, **11**(1), 8159.

Biabani, M., Fornito, A., Mutanen, T. P., Morrow, J., & Rogasch, N. C. (2019). Characterizing and minimizing the contribution of sensory inputs to TMS-evoked potentials. *Brain Stimulation*, **12**(6), 1537–1552.

Bonato, C., Miniussi, C., & Rossini, P. M. (2006). Transcranial magnetic stimulation and cortical evoked potentials: A TMS/EEG co-registration study. *Clinical Neurophysiology*, **117**(8), 1699–1707.

Boutros, N. N., Gjini, K., Urbach, H., & Pflieger, M. E. (2011). Mapping repetition suppression of the N100 evoked response to the human cerebral cortex. *Biological Psychiatry*, **69**(9), 883–889.

Bruckmann, S., Hauk, D., Roessner, V., Resch, F., Freitag, C. M., Kammer, T., Ziemann, U., Rothenberger, A., Weisbrod, M., & Bender, S. (2012). Cortical inhibition in attention deficit hyperactivity disorder: New insights from the electroencephalographic response to transcranial magnetic stimulation. *Brain*, **135**(7), 2215–2230.

Casali, A. G., Casarotto, S., Rosanova, M., Mariotti, M., & Massimini, M. (2010). General indices to characterize the electrical response of the cerebral cortex to TMS. *Neuroimage*, **49**(2), 1459–1468.

Che, X., Cash, R., Chung, S. W., Bailey, N., Fitzgerald, P. B., & Fitzgibbon, B. M. (2019). The dorsomedial prefrontal cortex as a flexible hub mediating behavioral as well as local and distributed neural effects of social support context on pain: A Theta Burst Stimulation and TMS-EEG study. *Neuroimage*, **201**, 116053.

Cheng, C. H., Chan, P. S., Hsieh, Y. W., & Chen, K. F. (2016). A meta-analysis of mismatch negativity in children with attention deficit-hyperactivity disorders. *Neuroscience Letters*, **612**, 132–137.

Chung, S. W., Lewis, B. P., Rogasch, N. C., Saeki, T., Thomson, R. H., Hoy, K. E., Bailey, N. W., & Fitzgerald, P. B. (2017). Demonstration of short-term plasticity in the dorsolateral prefrontal cortex with theta burst stimulation: A TMS-EEG study. *Clinical Neurophysiology*, **128**(7), 1117–1126.

Chung, S. W., Rogasch, N. C., Hoy, K. E., & Fitzgerald, P. B. (2015). Measuring brain stimulation induced changes in cortical properties using TMS-EEG. *Brain Stimulation*, **8**(6), 1010–1020.

Chung, S. W., Sullivan, C. M., Rogasch, N. C., Hoy, K. E., Bailey, N. W., Cash, R. F. H., & Fitzgerald, P. B. (2019). The effects of individualised intermittent theta burst stimulation in the prefrontal cortex: A TMS-EEG study. *Human Brain Mapping*, **40**(2), 608–627.

Conde, V., Tomasevic, L., Akopian, I., Stanek, K., Saturnino, G. B., Thielscher, A., Bergmann, T. O., & Siebner, H. R. (2019). The non-transcranial TMS-evoked potential is an inherent source of ambiguity in TMS-EEG studies. *Neuroimage*, **185**, 300–312.

Courchesne, E., Hillyard, S. A., & Galambos, R. (1975). Stimulus novelty, task relevance and the visual evoked potential in man. *Electroencephalography and Clinical Neurophysiology*, **39**(2), 131–143.

Darmani, G., Bergmann, T. O., Zipser, C., Baur, D., Muller-Dahlhaus, F., & Ziemann, U. (2019). Effects of antiepileptic drugs on cortical excitability in humans: A TMS-EMG and TMS-EEG study. *Human Brain Mapping*, **40**(4), 1276–1289.

Darmani, G., & Ziemann, U. (2019). Pharmacophysiology of TMS-evoked EEG potentials: A mini-review. *Brain Stimulation*, **12**(3), 829–831.

Donoghue, T., Haller, M., Peterson, E. J., Varma, P., Sebastian, P., Gao, R., Noto, T., Lara, A. H., Wallis, J. D., Knight, R. T., Shestyuk, A., & Voytek, B. (2020). Parameterizing neural power spectra into periodic and aperiodic components. *Nature Neuroscience*, **23**(12), 1655–1665.

Downar, J., Crawley, A. P., Mikulis, D. J., & Davis, K. D. (2002). A cortical network sensitive to stimulus salience in a neutral behavioral context across multiple sensory modalities. *Journal of Neurophysiology*, **87**(1), 615–620.

Du, X., Choa, F. S., Summerfelt, A., Rowland, L. M., Chiappelli, J., Kochunov, P., & Hong, L. E. (2017). N100 as a generic cortical electrophysiological marker based on decomposition of TMS-evoked potentials across five anatomic locations. *Experimental Brain Research*, **235**(1), 69–81.

Engel, A. K., & Fries, P. (2010). Beta-band oscillations–signalling the status quo? *Current Opinion in Neurobiology*, **20**(2), 156–165.

Fecchio, M., Pigorini, A., Comanducci, A., Sarasso, S., Casarotto, S., Premoli, I., Derchi, C. C., Mazza, A., Russo, S., Resta, F., Ferrarelli, F., Mariotti, M., Ziemann, U., Massimini, M., & Rosanova, M. (2017). The spectral features of EEG responses to transcranial magnetic stimulation of the primary motor cortex depend on the amplitude of the motor evoked potentials. *PLoS ONE*, **12**(9), e0184910.

Freedberg, M., Reeves, J. A., Hussain, S. J., Zaghloul, K. A., & Wassermann, E. M. (2020). Identifying site- and stimulation-specific TMS-evoked EEG potentials using a quantitative cosine similarity metric. *PLoS ONE*, **15**(1), e0216185.

Friedman, D., Cycowicz, Y. M., & Gaeta, H. (2001). The novelty P3: An event-related brain potential (ERP) sign of the brain's evaluation of novelty. *Neuroscience and Biobehavioral Reviews*, **25**(4), 355–373.

Gassmann, L., Gordon, P. C., & Ziemann, U. (2022). Assessing effective connectivity of the cerebellum with cerebral cortex using TMS-EEG. *Brain Stimulation*, **15**(6), 1354–1369.

Gordon, P. C., Desideri, D., Belardinelli, P., Zrenner, C., & Ziemann, U. (2018). Comparison of cortical EEG responses to realistic sham versus real TMS of human motor cortex. *Brain Stimulation*, **11**(6), 1322–1330.

Gordon, P. C., Jovellar, D. B., Song, Y., Zrenner, C., Belardinelli, P., Siebner, H. R., & Ziemann, U. (2021). Recording brain responses to TMS of primary motor cortex by EEG - utility of an optimized sham procedure. *Neuroimage*, **245**, 118708.

Gordon, P. C., Song, Y., Jovellar, B., Belardinelli, P., & Ziemann, U. (2023). No evidence for interaction between TMS-EEG responses and sensory inputs. *Brain Stimulation*, **16**(1), 25–27.

Grandchamp, R., & Delorme, A. (2011). Single-trial normalization for event-related spectral decomposition reduces sensitivity to noisy trials. *Frontiers in Psychology*, **2**, 236.

Groppa, S., Oliviero, A., Eisen, A., Quartarone, A., Cohen, L. G., Mall, V., Kaelin-Lang, A., Mima, T., Rossi, S., Thickbroom, G. W., Rossini, P. M., Ziemann, U., Valls-Sole, J., & Siebner, H. R. (2012). A practical guide to diagnostic transcranial magnetic stimulation: Report of an IFCN committee. *Clinical Neurophysiology*, **123**(5), 858–882.

Hall, S. D., Barnes, G. R., Furlong, P. L., Seri, S., & Hillebrand, A. (2010). Neuronal network pharmacodynamics of GABAergic modulation in the human cortex determined using pharmaco-magnetoencephalography. *Human Brain Mapping*, **31**(4), 581–594.

Hamalainen, M. S., & Ilmoniemi, R. J. (1994). Interpreting magnetic fields of the brain: Minimum norm estimates. *Medical & Biological Engineering & Computing*, **32**(1), 35–42.

Hannah, R., Muralidharan, V., & Aron, A. R. (2022). Motor cortex oscillates at its intrinsic post-movement beta rhythm following real (but not sham) single pulse, rhythmic and arrhythmic transcranial magnetic stimulation. *Neuroimage*, **251**, 118975.

Herring, J. D., Thut, G., Jensen, O., & Bergmann, T. O. (2015). Attention modulates TMS-locked alpha oscillations in the visual cortex. *Journal of Neuroscience*, **35**(43), 14435–14447.

Huguenard, J. R., & McCormick, D. A. (2007). Thalamic synchrony and dynamic regulation of global forebrain oscillations. *Trends in Neuroscience (Tins)*, **30**(7), 350–356.

Ilmoniemi, R. J., & Kicic, D. (2010). Methodology for combined TMS and EEG. *Brain Topography*, **22**(4), 233–248.

Kenemans, J. L. (2015). Specific proactive and generic reactive inhibition. *Neuroscience and Biobehavioral Reviews*, **56**, 115–126.

Ketz, N. A., Jensen, O., & O'Reilly, R. C. (2015). Thalamic pathways underlying prefrontal cortex-medial temporal lobe oscillatory interactions. *Trends in Neuroscience (Tins)*, **38**(1), 3–12.

Kiehl, K. A., Stevens, M. C., Laurens, K. R., Pearlson, G., Calhoun, V. D., & Liddle, P. F. (2005). An adaptive reflexive processing model of neurocognitive function: Supporting evidence from a large scale (n = 100) fMRI study of an auditory oddball task. *Neuroimage*, **25**(3), 899–915.

Komssi, S., & Kahkonen, S. (2006). The novelty value of the combined use of electroencephalography and transcranial magnetic stimulation for neuroscience research. *Brain Research Reviews*, **52**(1), 183–192.

Komssi, S., Kahkonen, S., & Ilmoniemi, R. J. (2004). The effect of stimulus intensity on brain responses evoked by transcranial magnetic stimulation. *Human Brain Mapping*, **21**(3), 154–164.

Lijffijt, M., Lane, S. D., Meier, S. L., Boutros, N. N., Burroughs, S., Steinberg, J. L., Moeller, F. G., & Swann, A. C. (2009). P50, N100, and P200 sensory gating: Relationships with behavioral inhibition, attention, and working memory. *Psychophysiology*, **46**(5), 1059–1068.

Lindhardt, K., Gizurarson, S., Stefansson, S. B., Olafsson, D. R., & Bechgaard, E. (2001). Electroencephalographic effects and serum concentrations after intranasal and intravenous administration of diazepam to healthy volunteers. *British Journal of Clinical Pharmacology*, **52**(5), 521–527.

Lioumis, P., Kicic, D., Savolainen, P., Makela, J. P., & Kahkonen, S. (2009). Reproducibility of TMS-Evoked EEG responses. *Human Brain Mapping*, **30**(4), 1387–1396.

Loheswaran, G., Barr, M. S., Zomorrodi, R., Rajji, T. K., Blumberger, D. M., Le Foll, B., & Daskalakis, Z. J. (2018). Alcohol impairs N100 response to dorsolateral prefrontal cortex stimulation. *Scientific Reports*, **8**(1), 3428.

Lozano-Soldevilla, D., ter Huurne, N., Cools, R., & Jensen, O. (2014). GABAergic modulation of visual gamma and alpha oscillations and its consequences for working memory performance. *Current Biology*, **24**(24), 2878–2887.

Maki, H., & Ilmoniemi, R. J. (2010). The relationship between peripheral and early cortical activation induced by transcranial magnetic stimulation. *Neuroscience Letters*, **478**(1), 24–28.

Massimini, M., Ferrarelli, F., Huber, R., Esser, S. K., Singh, H., & Tononi, G. (2005). Breakdown of cortical effective connectivity during sleep. *Science*, **309**(5744), 2228–2232.

Miller, E. K., Lundqvist, M., & Bastos, A. M. (2018). Working memory 2.0. *Neuron*, **100**(2), 463–475.

Mouraux, A., & Iannetti, G. D. (2009). Nociceptive laser-evoked brain potentials do not reflect nociceptive-specific neural activity. *Journal of Neurophysiology*, **101**(6), 3258–3269.

Nikouline, V., Ruohonen, J., & Ilmoniemi, R. J. (1999). The role of the coil click in TMS assessed with simultaneous EEG. *Clinical Neurophysiology*, **110**(8), 1325–1328.

Noda, Y., Barr, M. S., Zomorrodi, R., Cash, R. F. H., Rajji, T. K., Farzan, F., Chen, R., George, T. P., Daskalakis, Z. J., & Blumberger, D. M. (2018). Reduced short-latency afferent inhibition in prefrontal but not motor cortex and its association With executive function in Schizophrenia: A combined TMS-EEG study. *Schizophrenia Bulletin*, **44**(1), 193–202.

Oldfield, R. C. (1971). The assessment and analysis of handedness: the Edinburgh inventory. *Neuropsychologia*, **9**(1), 97–113.

Oostenveld, R., Fries, P., Maris, E., & Schoffelen, J. M. (2011). FieldTrip: Open source software for advanced analysis of MEG, EEG, and invasive electrophysiological data. *Computational Intelligence and Neuroscience*, **2011**, 156869.

Paus, T., Sipila, P. K., & Strafella, A. P. (2001). Synchronization of neuronal activity in the human primary motor cortex by transcranial magnetic stimulation: An EEG study. *Journal of Neurophysiology*, **86**(4), 1983–1990.

Pellicciari, M. C., Veniero, D., & Miniussi, C. (2017). Characterizing the cortical oscillatory response to TMS pulse. *Frontiers in Cellular Neuroscience*, **11**, 38.

Petrichella, S., Johnson, N., & He, B. (2017). The influence of corticospinal activity on TMS-evoked activity and connectivity in healthy subjects: A TMS-EEG study. *PLoS ONE*, **12**(4), e0174879.

Premoli, I., Bergmann, T. O., Fecchio, M., Rosanova, M., Biondi, A., Belardinelli, P., & Ziemann, U. (2017). The impact of GABAergic drugs on TMS-induced brain oscillations in human motor cortex. *Neuroimage*, **163**, 1–12.

Premoli, I., Biondi, A., Carlesso, S., Rivolta, D., & Richardson, M. P. (2017). Lamotrigine and levetiracetam exert a similar modulation of TMS-evoked EEG potentials. *Epilepsia*, **58**(1), 42–50.

Premoli, I., Castellanos, N., Rivolta, D., Belardinelli, P., Bajo, R., Zipser, C., Espenhahn, S., Heidegger, T., Muller-Dahlhaus, F., & Ziemann, U. (2014). TMS-EEG signatures of GABAergic neurotransmission in the human cortex. *Journal of Neuroscience*, **34**(16), 5603–5612.

Rangaswamy, M., & Porjesz, B. (2014). Understanding alcohol use disorders with neuroelectrophysiology. *Handbook of Clinical Neurology*, **125**, 383–414.

Rockstroh, B., Elbert, T., Lutzenberger, W., & Altenmuller, E. (1991). Effects of the anticonvulsant benzodiazepine clonazepam on event-related brain potentials in humans. *Electroencephalography and Clinical Neurophysiology*, **78**(2), 142–149.

Rogasch, N. C., Sullivan, C., Thomson, R. H., Rose, N. S., Bailey, N. W., Fitzgerald, P. B., Farzan, F., & Hernandez-Pavon, J. C. (2017). Analysing concurrent transcranial magnetic stimulation and electroencephalographic data: A review and introduction to the open-source TESA software. *Neuroimage*, **147**, 934–951.

Rogasch, N. C., Thomson, R. H., Farzan, F., Fitzgibbon, B. M., Bailey, N. W., Hernandez-Pavon, J. C., Daskalakis, Z. J., & Fitzgerald, P. B. (2014). Removing artefacts from TMS-EEG recordings using independent component analysis: Importance for assessing prefrontal and motor cortex network properties. *Neuroimage*, **101**, 425–439.

Romero, M. C., Davare, M., Armendariz, M., & Janssen, P. (2019). Neural effects of transcranial magnetic stimulation at the single-cell level. *Nature Communications*, **10**(1), 2642.

Rosburg, T. (2018). Auditory N100 gating in patients with schizophrenia: A systematic meta-analysis. *Clinical Neurophysiology*, **129**(10), 2099–2111.

Ross, J. M., Ozdemir, R. A., Lian, S. J., Fried, P. J., Schmitt, E. M., Inouye, S. K., Pascual-Leone, A., & Shafi, M. M. (2022). A structured ICA-based process for removing auditory evoked potentials. *Scientific Reports*, **12**(1), 1391.

Ross, J. M., Sarkar, M., & Keller, C. J. (2022). Experimental suppression of transcranial magnetic stimulation-electroencephalography sensory potentials. *Human Brain Mapping*.**43**(17), 5141–5153.

Russo, S., Sarasso, S., Puglisi, G. E., Dal Palu, D., Pigorini, A., Casarotto, S., D'Ambrosio, S., Astolfi, A., Massimini, M., Rosanova, M., & Fecchio, M. (2022). TAAC - TMS adaptable auditory control: A universal tool to mask TMS clicks. *Journal of Neuroscience Methods*, **370**, 109491.

Saletu, B., Grunberger, J., Linzmayer, L., Semlitsch, H. V., Anderer, P., & Chwatal, K. (1994). Pharmacokinetic and -dynamic studies with a new anxiolytic, suriclone, utilizing EEG mapping and psychometry. *British Journal of Clinical Pharmacology*, **37**(2), 145–156.

Schmidt, R., Herrojo Ruiz, M., Kilavik, B. E., Lundqvist, M., Starr, P. A., & Aron, A. R. (2019). Beta oscillations in working memory, executive control of movement and thought, and sensorimotor function. *Journal of Neuroscience*, **39**(42), 8231–8238.

Shader, R. I., Pary, R. J., Harmatz, J. S., Allison, S., Locniskar, A., & Greenblatt, D. J. (1984). Plasma concentrations and clinical effects after single oral doses of prazepam, clorazepate, and diazepam. *Journal of Clinical Psychiatry*, **45**(10), 411–413.

Singhal, A., Doerfling, P., & Fowler, B. (2002). Effects of a dual task on the N100-P200 complex and the early and late Nd attention waveforms. *Psychophysiology*, **39**(2), 236–245.

Stenroos, M., & Nummenmaa, A. (2016). Incorporating and compensating cerebrospinal fluid in surface-based forward models of magneto- and electroencephalography. *PLoS ONE*, **11**(7), e0159595.

Stenroos, M., & Sarvas, J. (2012). Bioelectromagnetic forward problem: Isolated source approach revis(it)ed. *Physics in Medicine and Biology*, **57**(11), 3517–3535.

Strobel, A., Debener, S., Sorger, B., Peters, J. C., Kranczioch, C., Hoechstetter, K., Engel, A. K., Brocke, B., & Goebel, R. (2008). Novelty and target processing during an auditory novelty oddball: A simultaneous event-related potential and functional magnetic resonance imaging study. *Neuroimage*, **40**(2), 869–883.

Tremblay, S., Rogasch, N. C., Premoli, I., Blumberger, D. M., Casarotto, S., Chen, R., Di Lazzaro, V., Farzan, F., Ferrarelli, F., Fitzgerald, P. B., Hui, J., Ilmoniemi, R. J., Kimiskidis, V. K., Kugiumtzis, D., Lioumis, P., Pascual-Leone, A., Pellicciari, M. C., Rajji, T., Thut, G., … Daskalakis, Z. J. (2019). Clinical utility and prospective of TMS-EEG. *Clinical Neurophysiology*, **130**(5), 802–844.

van Leeuwen, T. H., Verbaten, M. N., Koelega, H. S., Slangen, J. L., van der Gugten, J., & Camfferman, G. (1995). Effects of oxazepam on event-related brain potentials, EEG frequency bands, and vigilance performance. *Psychopharmacology*, **122**(3), 244–262.

Wessel, J. R., & Aron, A. R. (2017). On the globality of motor suppression: Unexpected events and their influence on behavior and cognition. *Neuron*, **93**(2), 259–280.

Zavala, B., Jang, A., Trotta, M., Lungu, C. I., Brown, P., & Zaghloul, K. A. (2018). Cognitive control involves theta power within trials and beta power across trials in the prefrontal-subthalamic network. *Brain*, **141**(12), 3361–3376.

Ziemann, U., Reis, J., Schwenkreis, P., Rosanova, M., Strafella, A., Badawy, R., & Muller-Dahlhaus, F. (2015). TMS and drugs revisited 2014. *Clinical Neurophysiology*, **126**(10), 1847–1868.

Additional information

Data availability statement

Data can be made available upon request.

MATLAB scripts, including the EEG pre-processing pipeline and statistics, are available at https://github.com/pcgordon/optimized_supraliminal_sham. These codes were designed for using the open-source toolbox Fieldtrip, version 20 210 212 (https://www.fieldtriptoolbox.org/).

Competing interests

U.Z. reports a grant from TAKEDA Millennium Pharmaceuticals, Inc., and personal consulting fees from CorTec GmbH, all outside the submitted work. All other authors declare no further competing financial interests.

Keywords

electroencephalography, GABA, inhibition, peripherally evoked potentials, pharmaco-TMS-EEG, sham stimulation, TMS-EEG, transcranial magnetic stimulation

Supporting information

Additional supporting information can be found online in the Supporting Information section at the end of the HTML view of the article. Supporting information files available:

Statistical Summary Document
Peer Review History